CBP manuscript 18932 - Part A

Cathepsin B differential expression and enzyme processing and activity during *Fundulus heteroclitus* embryogenesis

Angèle Tingaud-Sequeira [a,1], Oliana Carnevali [b], Joan Cerdà [a,*]

[a] *Laboratory of Institut de Recerca i Tecnologia Agroalimentàries (IRTA)-Institut de Ciències del Mar, Consejo Superior de Investigaciones Científicas (CSIC), 08003 Barcelona, Spain*

[b] *Department of Marine Sciences, Polytechnic University of Marche, Ancona, Italy*

* Corresponding author. Laboratory IRTA-Institut de Ciències del Mar (CSIC), Passeig marítim 37-49, 08003 Barcelona, Spain

E-mail address: joan.cerda@irta.cat (J. Cerdà).

[1] Now at Université Bordeaux 1, Génomique et Physiologie des Poissons, UMR NuAGe, 33405 Talence, France.

ABSTRACT

The role of lysosomal proteases such as cathepsin B (Ctsb) and one of the paralogs of cathepsin L (Ctsla) during yolk metabolism in fish oocytes is well established. However, the function of Ctsb during embryogenesis, particularly in marine teleosts, has been poorly documented. In this study, the spatio-temporal expression of Ctsb and Ctsla, their enzymatic activities, and the processing of the Ctsb and its cellular localization, was investigated in developing embryos of *F. heteroclitus*. Both *fhctsb* and *fhctsla* transcript levels, as well as cathepsin B- and L-like activities, gradually increased in embryos from the 2-4 cell stage up to 7 dpf. During the morula to gastrula transition an increase of the active FhCtsb single chain form was followed by a rise in cathepsin B activity, which were apparently regulated by post-transcriptional mechanisms. During neurulation, a 8-fold increase in cathepsin B activity was accompanied by a more moderate increase in cathepsin L activity, which was 6-fold enhanced by 7 days post-fertilization. These increased catalytic activities were well-correlated to changes in the electrophoretic pattern of yolk proteins and a strong expression of *fhctsb* and its protein product in the yolk syncytial layer. The increase of cathepsin B activity was further correlated with an increment of the relative amount of the FhCtsb single and double chain forms, both active forms of FhCtsb. These results suggest that FhCtsb may be involved in the mechanisms underlying the onset of gastrulation in *F. heteroclitus* embryos, and may play complementary roles with FhCtsla during yolk metabolism.

Key words: Embryo, yolk metabolism, gastrulation, cathepsin, enzyme processing

1. Introduction

Acidic proteases, generally known as cathepsins, are members of the endosomal/lysosomal protease family and now include more than 21 proteases (Roberts, 2005). They can be divided into four families according to the identity of the critical residue in the active site, cysteine, aspartate, serine, and metal ions in metalloprotease. Cathepsins are widely distributed in animal and plant tissues and in microorganisms, and are thought to play a wide range of biological functions, including protein turnover (Callegari et al., 2005), antigen processing (reviewed by Hsing and Rudensky, 2005), proenzyme activation (Azaryan and Hook, 1994), hormone maturation (Yasothornsrikul et al., 2003) or epidermal homeostasis (Roth et al., 2000, Tobin et al., 2002; Lecaille et al., 2002). In teleosts, the majority of cathepsins identified in mammals are also found (Carnevali et al., 1999a; Kwon et al., 2001; Fabra and Cerdà, 2004; Tan et al., 2006; Tingaud-Sequeira and Cerdà, 2007; Kao and Huang, 2008; Ahn et al., 2008, 2009; Yeh and Klesius, 2008, 2009; Jia and Zhang, 2009; Park et al., 2009; Je et al., 2009), and some of these are represented in the genome by duplicated or triplicated isoforms possibly as a result of the whole genome duplication event that occurred in the teleost lineage (Meyer and van de Peer, 2005). Thus, cathepsin B may remain in duplicate (Ctsba and Ctsbb) in some species (Tan et al., 2006; Tingaud- Sequeira and Cerdà, 2007), whereas cathepsin L may be present in triplicate (Ctsla, Ctslb, and Ctslc), as in the zebrafish (*Danio rerio*) (Tingaud- Sequeira and Cerdà, 2007). However, little information on the physiological functions of cathepsins in teleosts is yet available.

The role of cathepsins during yolk metabolism in fish has been however investigated more extensively (reviewed by Carnevali et al., 2006; Cerdà et al., 2007; Finn and Fyhn, 2010). Several cathepsins have been implicated in yolk processing, although experimental evidence is available only for a few of them. Thus, the aspartic protease cathepsin D (Ctsd) seems to be involved in the processing of the vitellogenins (Vtgs) into yolk proteins (YPs; lipovitellins, phosvitins, the β'-component, and the C-terminal peptide [Campbell and Idler, 1980; Matsubara and Sawano, 1995; Carnevali et al., 1999a]) in the oocyte during vitellogenesis (oocyte growth), whereas cysteine proteinases such as Ctsla, Ctsb and/or cathepsin Z (Ctsz) possibly participate in the subsequent hydrolysis of YPs during oocyte maturation (Sire et al., 1994; Carnevali et al., 1999b, 2008; Kwon et al., 2001; Hiramatsu et al., 2002; Matsubara et al., 2003; LaFleur et al., 2005; Raldúa et al., 2006; Kao and Huang, 2008). This additional cleavage of YPs produces a free amino acid (FAA) pool essential for the hydration of the oocytes, the subsequent buoyancy of spawned eggs in seawater, and as

energy source for developing embryos (Ohkubo and Matsubara, 2002; Cerdà et al., 2007; Finn, 2007a; Amano et al., 2008). However, the metabolism of Vtgs and YPs in the oocyte is most likely a complex and well coordinated process in which multiple cathepsins including Ctss, Ctsh and Ctsf may also be involved (Fabra and Cerdà, 2004; Raldúa et al., 2006; Kao and Huang, 2008).

Cathepsins also play a role during the mobilization and hydrolysis of the stored YPs in fish embryos, which is critical to embryonic development. Some studies have suggested that *ctsla*, which is maternally inherited and further highly expressed in the yolk syncytial layer (YSL) or periblast (Sire et al., 1994; Tingaud-Sequeira and Cerdà, 2007), may be the major protease in fish embryos and larvae (Murakami et al., 1990; Sire et al., 1994; Kestemont et al., 1999; Carnevali et al., 2001; Tingaud-Sequeira and Cerdà, 2007). The YSL consists of a vitellolysis zone and a cytoplasmic zone surrounding the yolk, and is therefore considered to play an integral role in the absorption of yolk in fish (Walzer and Schonënberger, 1979ab; Hemming and Buddington, 1988). The essential function of Ctsla in yolk hydrolysis during embryogenesis is further supported by the observation that genetic mutants of the *Caenorhabditis elegans* cathepsin L gene *cpl-1* show aberrant processing and/or conformational changes in YPs, resulting in abnormal yolk platelet fusion (Britton and Murray, 2004). In the zebrafish *ctsb* is also highly expressed in the YSL (Alt et al., 2006), and in some species of insects, the sea urchin and in salmonids, cathepsin B-like cysteine proteinases and/or serine proteases have been suggested as the enzymes involved in the processing of yolk materials during early embryogenesis (Mallya et al., 1992; Cho et al., 1999; Known et al., 2001; Hiramatsu et al., 2002). Therefore, it is possible that mechanisms for yolk processing during fish development are mediated by both Ctsla and Ctsb. However, the potential function of Ctsb, particularly in marine teleosts, has been poorly documented.

In the marine killifish *Fundulus heteroclitus*, which produces benthic eggs, a limited hydrolysis of YPs occurs during oocyte maturation, in which Ctsb rather than Ctsla is likely the major protease involved (LaFleur et al., 2005; Raldúa et al., 2006). In this species, there is no evidence for the expression of a second isoform of Ctsb in oocytes or embryos (Fabra and Cerdà, 2004). *F. heteroclitus* thus offers a good model to investigate the role of Ctsb during early development in fish. In the present study, we have determined the spatio-temporal changes in *F. heteroclitus ctsb* gene expression and enzyme activity during embryonic development in relation to those of Ctsla. These processes were correlated with developmental changes in the synthesis and processing of Ctsb and the occurrence of yolk proteolysis.

2. Materials and methods

2.1. Animals and embryo collection

Adult *F. heteroclitus* were obtained from saltmarshes in the bay of Cádiz (southern Spain), transported to the laboratory, and maintained as described (Cerdà et al., 1996; Fabra and Cerdà, 2004). Embryos were collected daily from naturally spawning fish using plastic trays placed at the bottom of the tanks (Tingaud-Sequeira et al., 2009), and were staged after Armstrong and Child (1965). Embryos were incubated in seawater (38‰ salinity; 1,110 mOsmol/kg H_2O) at 25ºC in a temperature-controlled incubator for up to 14-15 days post-fertilization (dpf), when most embryos hatched. Procedures related to the care and use of fish were approved by the Ethics Committee of the Institut de Recerca i Tecnologia Agroalimentàries (IRTA, Spain) in accordance with the "Guiding Principles for the Care and Use of Laboratory Animals".

2.2. Real-time quantitative PCR

The temporal expression pattern of *F. heteroclitus ctsb* (*fhctsb*) and *ctsla* (*fhctsla*) genes during embryonic development was assessed by real-time quantitative PCR (qPCR). Total RNA was extracted by using the RNAeasy minikit (Qiagen) and treated with Turbo-DNAse (Ambion) as indicated by the manufacturer. An aliquot corresponding to 1 µg was reverse transcribed using 0.5 µg oligo-$(dT)_{17}$, 1 mM dNTPs, 40 IU RNAse inhibitor, and 10 IU MMLuV-RT enzyme (Roche), for 1.5 h at 42ºC. Real-time PCR was performed with an ABI PRISM 7900HT Sequence Detection System (Applied Biosystems) using Power SYBR®Green PCR Master Mix (Applied Biosystems). For *fhctsb* (GenBank accession No. AY217741), the forward and reverse primers were 5'-GCTTAACACGACCTGGAAGG-3' and 5'-ACAGGAGCCTTGGTCTCTGA-3' (in exon 1 and 3, respectively, based on the genomic sequence of zebrafish *ctsba* gene). For *fhctsla* (GenBank accession No. AY212286), the forward and reverse primers were 5'-TGGAAGAGCTGGCACAGTAA-3' and 5'-TTTGTGCTTGTAGCCGTTCA-3' (in exon 1 and 3, respectively, based on the genomic sequence of zebrafish *ctsla* gene). *F. heteroclitus* ornithine decarboxylase (*odc*) mRNA (GenBank accession No. CN977303) was used as a reference gene, employing a forward primer 5'-GCTGCGTCCTCCACCTTCAT-3', and a reverse primer 5'-GGGCATGTCCAAGCTGCTCT-3' (Tingaud-Sequeira et al., 2009). The amplification reactions were carried out in a final volume of 20 µl, containing 10 µl of the master mix, 2 µl

of cDNA diluted 1:10 and 0.2 µM of each specific primer. The cycle was set as follows: activation for 120 s at 50°C and initial denaturation for 10 min at 95°C, followed by 40 cycles at 95°C for 10 s (denaturation) and 62°C for 60 s (annealing and extension). A final step with a decrease and increase of the temperature from 95°C to 60°C and from 60°C to 95°C, respectively, was applied to determine the melting curve. The threshold cycle number (Ct) was determined for all PCR reactions. Formation of primer dimmers was checked by adding water instead of the cDNA in the reaction mixture. The relative transcript level was calculated as fold change using the $2^{-\Delta\Delta Ct}$ method (Livak and Schmittgen, 2001).

2.3. Whole-mount in situ hybridisation

Whole-mount *in situ* hybridization on *F. heteroclitus* embryos was carried out as previously described (Tingaud-Sequeira and Cerdà, 2007). Digoxigenin (DIG)-labeled sense and antisense riboprobes were synthesized from the FhCtsb cDNA previously cloned (Fabra and Cerdà, 2004). Pre-hybridization and hybridization were carried out at 62ºC. After colorimetric reaction, embryos were transferred to glycerol solutions (25%, 50%, 75%, and then 100%), and pictures were taken on 100% glycerol-embedded embryos by using a Nikon SMZ1000 stereomicroscope. Some labeled embryos were transferred to 100% ethanol, then 100% xylol, and finally embedded into paraplast (Sigma) for sectioning. Sections (14 µm) were examined and photographed with a Zeiss Axioskop 2 plus microscope.

2.4. Cathepsin L- and B-like enzyme assays

Groups of embryos (n = 30) at different developmental stage were mechanically homogenized in 400 µl distilled water and the homogenate centrifuged at 14,000 x g for 10 min at 4ºC. The supernatant was recovered for each sample and the protein content measured using the Bio-Rad Protein Assay kit (Bio-Rad) using bovine serum albumin as standard. Cathepsin B- (EC 3.4.22.1) and L-like (EC 3.4.22.15) enzymatic activities were determined using the same colorimetric methods described by Zhang et al. (2008). For cathepsin B-like activity, Z-Arg-Arg-NNap (alpha-N-benzyloxycarbonyl-l-Arg-l-Arg-2-naphthylamide) was used as the specific synthetic substrate, whereas Z-Phe-Arg-NNapOMe in the presence of 4 M urea in the reaction buffer, which inhibits cathepsin B activity, was used to determine cathepsin L-like activity. The specific activity of cathepsin B-like was expressed as µmol of 2-naphthylamine released/min/mg of protein at 40ºC, whereas that of cathepsin L-like was expressed in µmol of 4-methoxy-2-naphthylamine released/min/mg of protein at 45°C. Each assay was repeated 3 times with different batches of embryos.

193

194 *2.5. SDS-PAGE of YPs*

195 Embryos at different developmental stages, 2-4 cells, morula, blastula, gastrula, neurula
196 and 7 pdf, were mechanically homogenized in 1 x Laemmli sample buffer (Laemmli, 1970)
197 and denatured at 95°C for 5 min. After treatment with 10 U of the endonuclease Benzonase
198 (Sigma) for DNA digestion (20 min at room temperature), the samples were centrifuged 10
199 min at full speed and processed for electrophoresis. A volume corresponding to 0.025 embryo
200 equivalents was loaded in each lane for YP profile determination. SDS-PAGE was performed
201 in 15% acrylamide minigels (7 x 3 x 10 cm) and electrophoresed at constant voltage (130 V)
202 for 1.5 h. After fixation in 12.5% trichloroacetic acid, the gel was stained overnight in 0.2%
203 Coomassie blue in 30% methanol and 10% acetic acid solution. The gel was progressively
204 destained in 25% methanol and 7% acetic acid solution until the bands were clearly revealed.
205 Previously identified YPs in *F. heteroclitus* oocytes and eggs (LaFleur et al., 2005) are related
206 to the precursor Vtg nomenclature proposed by Finn and Kristoffersen (2007) and Finn et al.
207 (2009).

208

209 *2.6. Immunoprecipitation and immunoblotting*

210 Ten embryos for each developmental stage (2-4 cell, morula, blastula, 50% epiboly, late
211 neurula, and 7 dpf) were homogenized on ice in 500 µL of NP-40-containing lysis buffer (1%
212 NP-40, 1 mM $CaCl_2$, 150 mM NaCl, 10 mM Tris-HCl pH 7.4) in PBS (137 mM NaCl, 2.7
213 mM KCl, 100 mM Na_2HPO_4, 2 mM KH_2PO_4, pH 7.4) supplemented with a cocktail of
214 protease inhibitors (mini-EDTA-free; Roche). Immunoprecipitation using 10 µg of anti-*F.*
215 *heteroclitus* Ctsb rabbit antiserum was performed as described (Raldúa et al., 2006). Aliquots
216 of 10 µg of immunoprecipitated protein for each embryo stage were separated by SDS-PAGE
217 (15%) and electroblotted onto PVDF membranes (Bio-Rad) using glycine transfer buffer (190
218 mM glycine, 25 mM Tris pH 8.6, 20% methanol). Membranes were blocked with TBST (20
219 mM Tris, 140 mM NaCl, 0.1% Tween, pH 7.6) containing 5% non-fat dry powder for 1 h,
220 and then incubated overnight with 1:500 diluted anti-*F. heteroclitus* Ctsb antisera in TBST
221 with 5% milk powder at 4°C. As secondary antibody, a 1:8000 dilution of goat anti-rabbit IgG
222 coupled to horseradish peroxidase (Sigma) was used. Reactive protein bands were detected
223 using enhanced chemiluminescence (Amersham). Three independent experiments on different
224 batches of embryos were performed for quantification of band intensity using the Gel Doc
225 software (Bio-Rad).

226

227 *2.7. Whole-mount immunocytochemistry*

228 Embryos were fixed in 4% paraformaldehyde (PFA) in PBS overnight at 4°C, and
229 subsequently washed in PBST (PBS, 0.8% Triton X-100) and manually dechorionated. After
230 five washes in PBST, non-specific sites were blocked by incubation in PBST containing 10%
231 goat serum for 2 h at room temperature. Embryos were transferred to 1% goat serum PBST
232 with anti-*F. heteroclitus* Ctsb antiserum diluted 1:500 and incubated overnight at 4°C.
233 Negative controls were probed with the antisera preincubated with 100 µg of the synthetic
234 peptide used for immunization (Raldúa et al., 2006) for 1 h at 37°C. After several washes of
235 15 min each with PBST, embryos were incubated with horseradish peroxidase conjugated
236 anti-rabbit IgG (1:200 diluted) in 1% goat serum PBST for 4 h at room temperature. Embryos
237 were washed with PBST and transferred to 0.1 M Tris pH 7.4 for 15 min. 3,3′-
238 Diaminobenzidine (DAB) revelation was performed as recommended by the manufacturer
239 (SIGMAFAST™, Sigma) until reactive signals were visible, and embryos were subsequently
240 stored in glycerol at 4ºC. For sectioning, embryos were washed with PBS containing
241 decreasing concentration of glycerol, dehydrated, and embedded into Paraplast. Sections (15
242 µm) were deparaffinized in xylene, mounted with Eukitt mounting medium (Fluka), and
243 photographed as indicated above.
244
245 *2.8. Immunofluorescence microscopy*

246 Chorion-bearing embryos at the gastrula stage (50-70% epiboly) were permeabilized
247 with 3% NaOCl for 1 min, and fixed with 4% PFA in PBS for 4 h at room temperature. After
248 fixation, embryos were manually dechorionated and refixed with 4 % PFA for 1 h. Embryos
249 were then washed, dehydrated and embedded into Paraplast. Sections (15 µm) were
250 rehydrated and blocked with 5 % goat serum in PBSTB (0.1% BSA, 0.05% Tween 20 in
251 PBS) for 1 h, and incubated with anti-*F. heteroclitus* Ctsb antisera (1:100) in 1% goat serum
252 PBSTB overnight at 4ºC. After washing, sections were incubated with a secondary anti-rabbit
253 IgG FITC-coupled antibody (Sigma) for 1 h, and subsequently with 4',6-diamidino-2-
254 phenylindole (DAPI; Sigma) diluted 1:3000 in PBS for 3 min. Sections were mounted with
255 fluoromount aqueous anti-fading medium (Sigma), and immunofluorescence was observed
256 and documented with a Zeiss imager.z1 microscope.
257
258 *2.9. Statistics*

259 The values presented are mean ± standard error of the mean (SEM). Data were analyzed
260 by one-way ANOVA followed by the Tukey's multiple-range test. When data were not

normally distributed, a non-parametric Kruskal-Wallis test, followed by a Mann-Whitney test, was used to detect statistical differences. Differences were considered significant at $p < 0.05$.

3. Results

3.1. Pattern of fhctsb and fhctsla gene expression during embryogenesis

The changes in *fhctsb* and *fhctsla* mRNA abundance from the 2-4-cell stage up to 7 dpf was determined by qPCR (Fig. 1). Expression of *fhctsb* and *fhctsla* was detected at the 2-4-cell stage indicating that both transcripts were maternally inherited. However, subsequent changes in the relative amount of *fhctsb* and *fhctsla* during development were different. The expression of *fhctsb* significantly ($p < 0.05$) dropped at the morula stage, presumably prior to the activation of zygotic expression, and progressively increased thereafter from the blastula stage until 7 dpf (Fig. 1A). In contrast, the levels of *fhctsla* remained unchanged until the blastula stage, increasing exponentially from the gastrula stage up to 7 dpf (Fig. 1B). However, the relative increase of *fhctsla* from the 2-4-cell stage up to 7 dpf was about the double of that of *fhctsb*.

To investigate the cellular localization of *fhctsb* expression during early embryogenesis, whole-mount *in situ* hybridization was carried out (Fig. 2). Contrary to the results obtained by qPCR, *fhctsb* transcripts could not be detected by *in situ* hybridization until the neurula stage, approximately at 24 h postfertilization (hpf) (Fig. 2A-C). By this time, a strong signal for *fhctsb* was obtained in the YSL surrounding the yolk sac (Fig. 2D-E), which remained through the 19-somite stage, approximately 48 hpf (Fig. 2F), up to 5 dpf (data not shown). The high level of *fhctsb* expression in the YSL was confirmed by immunolocalization of the protein product by whole-mount immunocytochemistry as well as by immunofluorescence microscopy using a specific anti-FhCtsb antiserum (Fig. 3). In both types of experiments, specific immunoreactions were seen in the cytoplasm of the YSL, whereas the more external blastomeres and the enveloping layer were negative (Fig. 3A).

3.2. Developmental heterochrony of cathepsin B- and L-like activities

In order to investigate if the pattern of *fhctsb* and *fhctsla* expression during embryo development correlated with differences in enzyme activation, cathepsin B- and L-like activities were assayed in embryos at different stages of development (Fig. 4). The developmental pattern observed for the cathepsin B-like activity approximately followed that of *fhctsb* expression. At the 2-4-cell stage, cathepsin B-like activity was very low and

progressively increased as the embryo developed from the morula stage, showing a 8-fold increase as embryos reached the neurula stage (Fig. 4A). Cathepsin B-like activity increased more moderately until 7 dpf, and then remained stable until the time of hatching, when a low but significant increase in activity was noted (Fig. 4). The changes in cathepsin L-like activity during development were delayed with respect those of cathepsin B-like (Fig. 4B). Thus, cathepsin L-like activity remained low until the gastrula stage and increased by about 2-fold at the neurula stage. By 7 dpf, a 6-fold elevation in activity was observed, which continued to increase until 14 dpf (Fig. 4B). Therefore, both cathepsin B- and L-like activities showed a marked increase (8- and 6-fold, respectively) during development, but that of cathepsin B-like occurred earlier.

3.3. Processing of FhCtsb during embryogenesis

To estimate the rate of FhCtsb synthesis and activation during embryonic development, Western blot analysis on immunoprecipitated FhCtsb was performed. In mammals, it is well established that cathepsin B is translated as a preproenzyme, and then transferred to the Golgi Complex as a proenzyme with very weak activity (reviewed by Ishidoh and Kominami, 2002). The mature cathepsin B enzyme is localized in lysosomes where it is found as both single and double chain forms. The double chain form is made up of two components originated from digestion of the single chain linked by disulfide bonds. In rats, peptide monomers of the procathepsin B form, the single chain active form, and the double chain form, have molecular masses of 45, 32 and 28 kDa, respectively (Authier et al., 1995). In the present study, three independent Western blots were performed to quantify the ratio between FhCtsb single chain and proFhCtsb (i.e., active and inactive forms, respectively). FhCtsb polypeptides were immunoprecipitated using the FhCtsb antiserum raised against the C terminus of the protein (Raldúa et al., 2006), which reduced further contamination with YPs and improved the immunodetection of FhCtsb.

The results of these experiments showed that just after fertilization (2-4 cell stage), three FhCtsb immunoreactive bands could be detected, which were identified as preproFhCtsb, proFhCtsb, and FhCtsb active single chain form, with apparent molecular masses of 47, 45 and 30 kDa, respectively (Fig. 5A). At the morula stage, a significant ($p < 0.05$) increase in the ratio of active FhCtsb single chain with respect the proenzyme was noted, but at subsequent blastula and gastrula stages the ratio decreased again to the levels observed in 2-4-cell embryos (Fig. 5B). By the neurula stage, a significant ($p < 0.05$) increase of the active FhCtsb single chain form with respect to the proenzyme was further observed

(Fig. 5B), and a fourth 28 kDa immunoreactive band, most likely corresponding to the FhCtsb heavy chain of the double chain form, became apparent (Fig. 5A). By 7 dpf, the FhCtsb double chain form appeared to increase, whereas the single chain FhCtsb form was almost double that of the proenzyme (Fig. 5B). These data thus positively correlated with the increased cathepsin B-like activity observed from the gastrula stage up to 7 dpf.

3.4. Pattern of YP hydrolysis during F. heteroclitus embryo development

To investigate if the changes in FhCtsb and FhCtsla gene expression and enzyme processing and activity correlated with yolk proteolysis during embryogenesis, the changes in the major YPs were characterized by SDS-PAGE followed by Coomassie blue staining (Fig. 6). In 2-4-cell embryos, a total of 11 different bands were revealed by SDS-PAGE, which were named after their apparent molecular mass. Nine of these YPs, YP122, YP103, YP77, YP75, YP69, YP45, YP42, YP26 and YP19, have been reported in *F. heteroclitus* unfertilized eggs (Lafleur et al., 2005), whereas the YP50 and YP32, which seems to be absent before fertilization, appeared as a very tiny bands. No major band shifts were detected until the neurula stage, when the YP122 completely disappeared, and a new YP with an apparent molecular mass of approximately 25 kDa was detected (Fig. 6). At the same time, the amount of YP103 decreased slightly, which corresponded to an increased intensity of YP77. These altered electrophoretic profiles during neurulation correlated well with the 10-fold increase in cathepsin B-like activity. By 7 dpf, when the activities of both cathepsin B- and L-like were almost asymptotic, the hydrolysis of YPs was more pronounced. At this stage, a marked decrease of the YP103 and YP69 bands, and increase of the YP77 band was, observed, while the YP25 band, which originated by the neurula stage, and the YP42 band disappeared. Concomitantly, newly formed YPs, YP40, YP22, YP21, YP18 and YP15, were detected, as well as an increase of the intensity of the YP32 band and a decrease of that of YP19. The YP50 and YP45 remained essentially unaltered at 7 dpf.

4. Discussion

By using N-terminal microsequencing of isolated YPs, Lafleur et al., (2005) described the model of Vtg/YP precursor/product relationship and further processing during oocyte maturation in *F. heteroclitus*, which may be similar for other teleosts producing benthic eggs (LaFleur et al., 2005; Cerdà et al., 2007; Finn, 2007b). Thus, in *F. heteroclitus* most of the YPs identified in post-vitellogenic oocytes are derived from VtgAa (Vtg1), whereas YP69 is

363 originated from the hydrolysis of VtgAb (Vtg2), which is also proteolytically cleaved into
364 small peptides during vitellogenesis (LaFleur et al., 2005). During the transformation of
365 oocytes into mature, ovulated eggs, one of the most pronounced changes in the oocyte YPs is
366 the drastic reduction of the YP122, which corresponds to the heavy chain of VtgAa
367 lipovitellin (Wallace and Begovac, 1985; Wallace and Selman, 1985; Greeley et al., 1986;
368 McPherson et al., 1989; LaFleur et al., 2005), while YP45 is partially degraded (LaFleur et
369 al., 2005). In the present study we show that no major YP proteolysis occurs until after
370 gastrulation. Thereafter, significant proteolysis commences during neurulation and becomes
371 more prominent by 7 dpf. Interestingly, the VtgAb-derived YP69 was maintained more or less
372 intact until 7 dpf, suggesting that VtgAa-derived YPs are the initial nutritive sources during *F.*
373 *heteroclitus* early embryogenesis. Nevertheless, the delay in yolk resorption during
374 embryogenesis, which in *F. heteroclitus* was not detected until 24 hpf, has also been
375 described in salmonids such as masu salmon (*Oncorhynchus masou*) and Sakhalin taimen
376 (*Hucho perryi*) in which proteolysis of YPs does not occur until mid-embryogenesis, by 14
377 and 22 dpf, respectively (Hiramatsu *et al.*, 2002). In barfin flounder (*Verasper moseri*),
378 utilization of VtgAb-derived lipovitellin occurs also late from 16 dpf, and correlates with the
379 depletion of the FAA pool originated from the hydrolysis of YPs during oocyte maturation
380 (Ohkubo and Matsubara, 2002), suggesting that amino acids from the YP pool are recruited
381 when the FAA pool cannot fulfill anymore the nutritional requirements of developing
382 embryos (Finn et al., 1996; Ohkubo and Matsubara, 2002; Finn and Fyhn, 2010). A similar
383 scenario may be proposed for *F. heteroclitus* embryos, although some hydrolysis of YPs
384 occurring at earlier stages producing peptides that do not appear on the gels as bands either
385 because they do not stain well with Coomassie blue or because they are too small to resolve
386 on the gel, cannot be ruled out.
387 Since FhCtsb has been suggested as the major enzyme involved in the oocyte
388 maturation-associated proteolytic processing of YP122 in *F. heteroclitus* (LaFleur et al.,
389 2005), in the present study we investigated in detail developmental changes in *fhctsb* gene
390 expression and enzyme activity. In comparison, we also determined the changes in *fhctsla*
391 expression and cathepsin L-like activity since this protease is likely to be involved in yolk
392 proteolysis during fish embryogenesis (Murakami et al., 1990; Sire et al., 1994; Kestemont et
393 al., 1999; Carnevali et al., 2001; Tingaud-Sequeira and Cerdà, 2007). Our data indicate that
394 both *fhctsb* and *fhctsla* transcripts in embryos progressively increased during development
395 from the 2-4 cell stage up to 7 dpf. Accordingly, cathepsin B- and L-like activities increased
396 with development, but a 8-fold increase in cathepsin B activity, which was accompanied by a

more moderate increase in cathepsin L activity, was observed at the neurula stage, when hydrolysis of YPs start to be visible. Such an increase of cathepsin B activity correlated with an increment in the embryo of the relative amount of the active FhCtsb single chain form with respect to the proenzyme. These observations, together with the fact that *fhctsb* and the protein product are strongly expressed in the YSL, suggest that FhCtsb, possibly together with Ctsla, may play a role in the initial mechanisms of yolk resorption in *F. heteroclitus*.

Western blot analysis of immunoprecipitated FhCtsb also revealed that this protease possibly acts in two-chain form as described for mammals and in teleosts such as the common carp (*Cyprinus carpio*) (Ishidoh and Kominami, 2002; Tan et al., 2006). This notion is strengthened by comparing the amino acid sequences flanking the cleavage site between the light chain and heavy chain of mammalian, common carp and *F. heteroclitus* cathepsin B, in which a basic residue and a Val are conserved (Arg^{49}-Val^{50} in mouse and bovine cathepsin B [Ferrara et al., 1990; Bechet et al., 1991], and Lys^{49}-Val^{50} in carp and *F. heteroclitus* cathepsin B [Fabra and Cerdà, 2004; Tan et al., 2006]). In common carp muscle, the N-terminal amino acid sequence of the putative Ctsb heavy chain shows high homology with those of mammalian cathepsin B, suggesting that the common carp Ctsb most likely works in two-chain form, consisting of a light chain and a heavy chain bound by disulfide bond (Tan et al., 2006). In contrast, common carp and *F. heteroclitus* Ctsla are likely to act only as single chain forms since the P1 position at the cleavage site, which contains a hydrophylic amino acid (Ser) in mammalian cathepsin L, is a hydrophobic residue (Val) in both common carp and *F. heteroclitus* Ctsla (Fabra and Cerdà, 2004; Tan et al., 2006). The appearance of the FhCtsb double chain form in embryos occurred at neurula stage and appeared to increase later in development, being however absent at earlier stages. The physiological significance of this differential processing of FhCtsb during embryogenesis remains intriguing and requires further investigation.

A heterochronic increase in cathepsin B-like activity, but not of cathepsin L-like activity was observed from the blastula stage, and was preceded by an elevation of the active form of FhCtsb at the morula stage. The elevation of both FhCtsb active form and further enzyme activity may have been derived from maternal mRNA, but later it was likely regulated by post-transcriptional mechanisms, since the *fhctsb* transcript levels in the embryo markedly decreased at the morula and blastula stages. The levels of maternal *fhctsb*, which are reported to be accumulated in ovarian follicles throughout vitellogenesis (Fabra and Cerdà, 2004), were apparently quite low during early embryogenesis since they could only be detected by qPCR. Maternal levels of *fhctsb* therefore may be much lower than those of *fhctsla* which

have been shown to increase approximately by 3-fold during oocyte maturation (Fabra and Cerdà, 2004) and are highly expressed at the morula stage of *F. heteroclitus* and zebrafish (Tingaud-Sequeira and Cerdà, 2007). Nevertheless, the specific activation of FhCtsb during the blastula and gastrula stages suggest that maternal *fhctsb* may play a critical function in *F. heteroclitus* early embryos unrelated to yolk mobilization. In European sea bass (*Dicentrarchus labrax*), maximum cathepsin B activity occurs at the morula stage (Carnevali et al., 2001), which may be a consequence of the different development rates of these embryos when compared with those of *F. heteroclitus* (e.g. European sea bass embryos hatch at about 2 dpf at 16-17ºC [Devauchelle and Coves, 1988], whereas water-immersed *F. heteroclitus* embryos hatch at 14-15 dpf at 25ºC [e.g., Tingaud-Sequeira et al., 2009]).

It is well established that proteases play distinct roles in the processing of signalling molecules involved in mesodermal patterning in various embryos (Yajima and Kawashima, 2002; Blomberg et al., 2008). Thus, for instance, precursor molecules of latent transforming growth factor beta (TGF-β) have been reported to be activated by lysosomal proteases (Oursler et al., 1993), and the receptor for the platelet-derived growth factor (PDGF), which is involved in pathways controlling the migration, differentiation and function of a variety of specialized mesenchymal and migratory cell types during gastrulation (Hoch and Soriano, 2003), is cleaved by a thiol protease to enable it to bind PDGF (Ek and Heldin, 1986). In *Xenopus laevis* embryos, disruption of cathepsin L with an antibody against cathepsin L-like protease induces a defective gastrulation leading to an abnormal mesodermal structure (Miyata and Kubo, 1997). Therefore, it is possible that the activation of FhCtsb and gradual increment of its activity during the blastula and gastrula stages in *F. heteroclitus* embryos are related with a role of this protease at the onset of gastrulation. However, it has been reported that Ctsb may regulate the activation of cathepsin L- and caspase-3-like activity in zebrafish ovarian follicles (Carnevali et al., 2006; Eykelbosh and Van der Kraak, 2010), and consequently whether the action of Ctsb on embryonic signalling pathways is direct or through the activation of other proteases such as Ctsla is unknown.

In summary, this study provides evidence for the potential role of FhCtsb during gastrulation and yolk metabolism in *F. heteroclitus* embryos. The present observations that stage-specific yolk proteolysis coincides with increased activity of FhCtsla, which is also expressed in the YSL of developing embryos (Tingaud-Sequeira and Cerdà, 2007), suggest that FhCtsla plays a complementary catalytic role to that of FhCtsb during yolk mobilization. Wheather the specific role of Ctsb in this mechanism is the activation of Ctsla (Carnevali et al., 2006) remains to be investigated. However, in other teleosts, such as the zebrafish, *ctss*

and *ctsc* mRNAs are also localized in the embryonic YSL (Thisse et al., 2001; Rauch et al., 2003). These findings thus suggest that yolk degradation during embryogenesis in teleosts may possibly require the combined action of different proteolytic enzymes in addition to Ctsb and Ctsla (Sire et al., 1994; Hiramatsu et al., 2002). Further studies will be necessary to elucidate the specific role of the different embryonic cathepsins including Ctsb, as well as their interactions, during early embryogenesis and yolk metabolism in teleosts.

Acknowledgments

We thank Dr. F. Chauvigné for his assistance during the immunocytochemical procedures, and Dr. R. N. Finn for critically reading the manuscript. This work was financed by grants from the Spanish Ministry of Science and Innovation (MICINN, AGL2004-00316 and HI2002-0051) to JC, and by a bilateral project Italy-Spain (Azioni Integrate Italia Spagna IT 1021 a.f. 2003) to OC.

References

Ahn, S.J., Kim, N.Y., Jeon, S.J., Sung, J.H., Je, J.E., Seo, J.S., Kim, M.S., Kim, J.K., Chung, J.K., Lee, H.H., 2008. Molecular cloning, tissue distribution and enzymatic characterization of cathepsin X from olive flounder (*Paralichthys olivaceus*). Comp. Biochem. Physiol. B 151, 203-212.

Ahn, S.J., Kim, N.Y., Seo, J.S., Je, J.E., Sung, J.H., Lee, S.H., Kim, M.S., Kim, J.K., Chung, J.K., Lee, H.H., 2009. Molecular cloning, mRNA expression and enzymatic characterization of cathepsin F from olive flounder (*Paralichthys olivaceus*). Comp. Biochem. Physiol. B 154, 211-220.

Alt, B., Reibe, S., Feitosa, N.M., Elsalini, O.A., Wendl, T., Rohr, K.B., 2006. Analysis of origin and growth of the thyroid gland in zebrafish. Dev. Dyn. 235, 1872-1883.

Amano, H., Fujita, T., Hiramatsu, N., Kagawa, H., Matsubara, T., Sullivan, C.V., Hara, A., 2008. Multiple vitellogenin-derived yolk proteins in gray mullet (*Mugil cephalus*): disparate proteolytic patterns associated with ovarian follicle maturation. Mol. Reprod. Dev. 75, 1307-1317.

Armstrong, P.B., Child, J.W., 1965. Stages in the normal development of *Fundulus heteroclitus*. Biol. Bull. 128, 143-168.

498 Authier, F., Mort, J.S., Bell, A.W., Posner, B.I., Bergeron, J.J., 1995. Proteolysis of glucagon within
499 hepatic endosomes by membrane-associated cathepsins B and D. J. Biol.Chem., 270, 15798-
500 15807.
501 Azaryan, A.V, Hook, V.Y., 1994. Unique cleavage specificity of 'prohormone thiol protease' related to
502 proenkephalin processing. FEBS Lett. 341, 197-202.
503 Bechet, D.M., Ferrara, M.J., Mordier, S.B., Roux, M.P., Deval, C.D., Obled, A., 1991. Expression of
504 lysosomal cathepsin B during calf myoblast-myotube differentiation. Characterization of a
505 cDNA encoding bovine cathepsin B. J. Biol. Chem. 266, 14104-14112 .
506 Blomberg, L., Hashizume, K., Viebahn, C., 2008. Blastocyst elongation, trophoblastic differentiation,
507 and embryonic pattern formation. Reproduction 135, 181-195.
508 Britton, C., Murray, L., 2004. Cathepsin L protease (CPL-1) is essential for yolk processing during
509 embryogenesis in *Caenorhabditis elegans*. J. Cell Sci. 117, 5133-5143.
510 Callegari, E.A., Ferguson-Gottschall, S., Gibori, G., 2005. PGF2alpha induced differential expression
511 of genes involved in turnover of extracellular matrix in rat decidual cells. Reprod. Biol.
512 Endocrinol. 3, 3.
513 Campbell, C.M, Idler, D.R., 1980. Characterization of an estradiol-induced protein from rainbow trout
514 serum as vitellogenin by the composition and radioimmunological cross reactivity to ovarian
515 yolk fractions. Biol. Reprod. 22, 605-617.
516 Carnevali, O., Centonze, F., Brooks, S., Marota, I., Sumpter, J.P., 1999a. Molecular cloning and
517 expression of ovarian cathepsin D in seabream, *Sparus aurata*. Biol. Reprod. 61, 785-791.
518 Carnevali, O., Carletta, R., Cambi, A., Vita, A., Bromage, N., 1999b. Yolk formation and degradation
519 during oocyte maturation in seabream *Sparus aurata*. Involvement of two lysosomal
520 proteinases. Biol. Reprod. 60, 140–146.
521 Carnevalli, O., Mosconi, G., Cambi, A., Ridolfi, S., Zanuy, S., Polzonetti-Magni, A.M., 2001.
522 Changes of lysosomal enzyme activities in sea bass (*Dicentrarchus labrax*) eggs and developing
523 embryos. Aquaculture 202, 249-256.
524 Carnevali, O., Cionna, C., Tosti, L., Lubzens, E., Maradonna, F., 2006. Role of cathepsins in ovarian
525 follicle growth and maturation. Gen. Comp. Endocrinol. 146, 195-203.
526 Carnevali, O., Cionna, C., Tosti, L., Cerdà, J., Gioacchini, G., 2008. Changes in cathepsin gene
527 expression and relative enzymatic activity during gilthead sea bream oogenesis. Mol. Reprod.
528 Dev. 75, 97-104.
529 Cerdà, J., Calman, B.G., LaFleur, G.J. Jr., Limesand, S., 1996. Pattern of vitellogenesis and follicle
530 maturational competence during the ovarian follicular cycle of *Fundulus heteroclitus*. Gen.
531 Comp. Endocrinol. 103, 24-35.
532 Cerdà, J., Fabra, M., Raldúa, D., 2007. Physiological and molecular basis of fish oocyte hydration. In:
533 Babin, P., Cerdà, J., Lubzens, E. (Eds.), The Fish Oocyte: from Basic Studies to
534 Biotechnological Applications. Springer-Verlag, The Netherlands, pp. 349-396.

535 Cho, W.L., Tsao, S.M., Hays, A.R., Walter, R., Chen, J.S., Snigirevskaya, E.S., Raikhel, A.S., 1999.
536 Mosquito cathepsin B-like protease involved in embryonic degradation of vitellin is produced as
537 a latent extraovarian precursor. J. Biol Chem 274, 13311-13321.
538 Devauchelle, N., Coves, D., 1988. The characteristics of sea bass (*Dicentrarchus labrax*) eggs:
539 Description, biochemical composition and hatching performances. Aquat. Liv. Resourc. 1:223-
540 230.
541 Ek, B., Heldin, C.H., 1986. Specific cleavage of the fibroblast receptor for platelet-derived growth
542 factor by an endogenous Ca^{2+}-dependent thiol protease. Eur. J. Biochem. 155, 409-413.
543 Eykelbosh, A.J., Van Der Kraak, G., 2010. A role for the lysosomal protease cathepsin B in zebrafish
544 follicular apoptosis. Comp. Biochem. Physiol. A 156, 218-223.
545 Fabra, M., Cerdà, J., 2004. Ovarian cysteine proteinases in the teleost *Fundulus heteroclitus*:
546 molecular cloning and gene expression during vitellogenesis and oocyte maturation. Mol.
547 Reprod. Dev. 67, 282-294.
548 Ferrara, M., Wojcik, F., Rhaissi, H., Mordier, S., Roux, M.-P., Bechet, D., 1990. Gene structure of
549 mouse cathepsin B. FEBS Lett. 273, 195-199.
550 Finn, R.N., Fyhn, H.J., Henderson, R.J., Evjen, M.S., 1996. The sequence of catabolic substrate
551 oxidation and enthalpy balance of developing embryos and yolk-sac larvae of turbot
552 (*Scophthalmus maximus* L.). Comp. Biochem. Physiol. A 115, 133-151.
553 Finn, R.N., 2007a. The maturational disassembly and differential proteolysis of paralogous
554 vitellogenins in a marine pelagophil teleost: a conserved mechanism of oocyte hydration. Biol.
555 Reprod. 76, 936-948.
556 Finn, R.N., 2007b. Vertebrate yolk complexes and the functional implications of phosvitins and other
557 subdomains in vitellogenins. Biol. Reprod. 76, 936-948.
558 Finn, R.N., Kristoffersen, B.A., 2007. Vertebrate vitellogenin gene duplication in relation to the ‘‘3R
559 Hypothesis’’: Correlation to the pelagic egg and the oceanic radiation of teleosts. PLoS ONE 2,
560 e169.
561 Finn, R.N., Kolarevic, J., Kongshaug, H., Nilsen, F., 2009. Evolution and differential expression of a
562 vertebrate vitellogenin gene cluster. BMC Evol. Biol. 9, 2.
563 Finn, R.N., Fyhn, H.J., 2010. Requirement for amino acids in ontogeny of fish. Aquaculture Res. 41,
564 684-716.
565 Greeley, M.S. Jr., Calder, D.R., Wallace, R.A., 1986. Changes in teleost yolk proteins during oocyte
566 maturation: correlation of yolk proteolysis with oocyte hydration. Comp. Biochem. Physiol. B
567 84, 1-9.
568 Heming, T.A., Buddington, R.K., 1988. Yolk absorption in embryonic and larval fishes. In: Hoar,
569 W.S., Randall, D.J. (Eds), Fish Physiology, vol 11A. Academic press, New York, pp. 407-446.

570 Hiramatsu, N., Ichikawa, N., Fukada, H., Fujita, T., Sullivan, C.V., Hara, A., 2002. Identification and
571 characterization of proteases involved in specific proteolysis of vitellogenin and yolk proteins in
572 salmonids. J. Exp. Zool. 292, 11-25.
573 Hoch, R.V., Soriano, P., 2003. Roles of PDGF in animal development. Development 130, 4769-4784.
574 Hsing, L.C., Rudensky, A.Y., 2005. The lysosomal cysteine proteases in MHC class II antigen
575 presentation. Immunol. Rev. 207, 229-241.
576 Ishidoh, K., Kominami, E., 2002. Processing and activation of lysosomal proteinases. Biol. Chem.
577 383, 1827-1831.
578 Kao, C.M., Huang, F.L., 2008. Cloning and expression of carp cathepsin Z: possible involvement in
579 yolk metabolism. Comp Biochem Physiol B 149, 541-551.
580 Kestemont, P., Cooremans, J., Abi-Ayad, A., Mélard, C., 1999. Cathepsin L in eggs and larvae of
581 perch Perca fluviatilis: variations with developmental stage and spawning period. Fish Physiol.
582 Biochem. 21, 59-64.
583 Kwon, J.Y., Prat, F., Randall, C., Tyler, C.R., 2001. Molecular characterization of putative yolk
584 processing enzymes and their expression during oogenesis and embryogenesis in rainbow trout
585 (*Oncorhynchus mykiss*). Biol. Reprod. 65, 1701-1709.
586 Je, J.E., Ahn, S.J., Kim, N.Y., Seo, J.S., Kim, M.S., Park, N.G., Kim, J.K., Chung, J.K., Lee, H.H.,
587 2009. Molecular cloning, expression analysis and enzymatic characterization of cathepsin K
588 from olive flounder (*Paralichthys olivaceus*). Comp. Biochem. Physiol. A 154, 474-485.
589 Jia, A., Zhang, X.H., 2009. Molecular cloning, characterization and expression analysis of cathepsin D
590 gene from turbot *Scophthalmus maximus*. Fish Shellfish Immunol. 26, 606-613.
591 Laemmli, U.K., 1970. Cleavage of structural proteins during the assembly of the head of
592 bacteriophage T4. Nature 227, 680-685.
593 LaFleur, G.J. Jr., Raldúa, D., Fabra, M., Carnevali, O., Denslow, N., Wallace, R.A., Cerdà, J., 2005.
594 Derivation of major yolk proteins from parental vitellogenins and alternative processing during
595 oocyte maturation in *Fundulus heteroclitus*. Biol. Reprod. 73, 815-824.
596 Livak, K.J., Schmittgen, T.D., 2001. Analysis of relative gene expression data using real-time
597 quantitative PCR and the 2(-Delta Delta C(T)) method. Methods 25, 402-408.
598 McPherson, R., Greeley, M.S. Jr., Wallace, R.A., 1989. The influence of yolk protein proteolysis on
599 hydration in the oocytes of *Fundulus heteroclitus*. Dev. Growth Differ. 31, 475-483.
600 Mallya, S., Partin, J.S., Valdizan, M.C., Lennarz, W.J., 1992. Proteolysis of the major yolk
601 glycoproteins is regulated by acidification of the yolk platelets in sea urchin embryos. J. Cell
602 Biol. 117, 1211-1221.
603 Matsubara, T., Sawano, K., 1995. Proteolytic cleavage of vitellogenin and yolk proteins during
604 vitellogenin uptake and oocyte maturation in barfin flounder (*Verasper moseri*). J. Exp. Zool.
605 272, 34-45.

606 Matsubara, T., Nagae, M., Ohkubo, N., Andoh, T., Sawaguchi, S., Hiramatsu, N., Sullivan, C.V.,
607 Hara, A., 2003. Multiple vitellogenins and their unique roles in marine teleosts. Fish Physiol.
608 Biochem. 28, 295-299.
609 Meyer, A., Van de Peer, Y., 2005. From 2R to 3R: evidence for a fish-specific genome duplication
610 (FSGD). Bioessays 27, 937-945.
611 Miyata, S., Kubo, T., 1997. Inhibition of gastrulation in *Xenopus* embryos by an antibody against a
612 cathepsin L-like protease. Dev. Growth Differ. 39, 111-115.
613 Murakami, M., Iuchi, I., Yamagami, K., 1990. Yolk phosphoprotein metabolism during early
614 development of the fish, *Oryzias latipes*. Dev. Growth Differ. 32, 619-627.
615 Ohkubo, N., Matsubara, T., 2002. Sequential utilization of free amino acids, yolk proteins and lipids in
616 developing eggs and yolk-sac larvae of barfin flounder *Verasper moseri*. Mar. Biol. 140, 187-
617 196.
618 Oursler, M.J., Riggs, B.L., Spelsberg, T.C., 1993. Glucocorticoid-induced activation of latent
619 transforming growth factor-beta by normal human osteoblast-like cells. Endocrinology 133,
620 2187-2196.
621 Park, E.M., Kim, Y.O., Nam, B.H., Kong, H.J., Kim, W.J., Lee, S.J., Kim, K.K., 2009. Cloning and
622 expression analysis of cathepsin D in the olive flounder *Paralichthys olivaceus*. Biosci.
623 Biotechnol. Biochem. 73, 1856-1859.
624 Raldúa, D., Fabra, M., Bozzo, M.G., Weber, E., Cerdà, J., 2006. Cathepsin B-mediated yolk protein
625 degradation during killifish oocyte maturation is blocked by an H^+-ATPase inhibitor: effects on
626 the hydration mechanism. Am. J. Physiol. Regul. Integr. Comp. Physiol. 290, R456-R466.
627 Rauch, G.J., Lyons, D.A., Middendorf, I., Friedlander, B., Arana, N., Reyes, T., Talbot, W.S., 2003.
628 Submission and Curation of Gene Expression Data. ZFIN Direct Data Submission.
629 Roberts, R., 2005. Lysosomal cysteine proteases: structure, function and inhibition of cathepsins. Drug
630 News Perspect. 18, 605-614.
631 Sire, M.F., Babin, P.J., Vernier, J.M., 1994. Involvement of the lysosomal system in yolk protein
632 deposit and degradation during vitellogenesis and embryonic development in trout. J. Exp. Zool.
633 269, 69-83.
634 Tan, Y., Osatomi, K., Nozaki, Y., Ishihara, T., Hara, K., 2006. Occurrence of two distinct molecular
635 species of cathepsin B in carp. Fish. Sci. 72, 185-194.
636 Thisse, B., Pflumio, S., Fürthauer, M., Loppin, B., Heyer, V., Degrave, A., Woehl, R., Lux, A.,
637 Steffan, T., Charbonnier, X.Q., Thisse, C., 2001. Expression of the zebrafish genome during
638 embryogenesis (NIH R01 RR15402). ZFIN Direct Data Submission.
639 Tingaud-Sequeira, A., Cerdà, J., 2007. Phylogenetic relationships and gene expression pattern of three
640 different cathepsin L (Ctsl) isoforms in zebrafish: Ctsla is the putative yolk processing enzyme.
641 Gene 386, 98-106.

642 Tingaud-Sequeira, A., Zapater, C., Chauvigne, F., Otero, D., Cerdà, J., 2009. Adaptive plasticity of
643 killifish (*Fundulus heteroclitus*) embryos: dehydration-stimulated development and differential
644 aquaporin-3 expression. Am. J. Physiol. Regul. Integr. Comp. Physiol. 296, R1041-R1052.
645 Tobin, D.J., Foitzik, K., Reinheckel, T., Mecklenburg, L., Botchkarev, V.A., Peters, C., Paus, R.,
646 2002. The lysosomal protease cathepsin L is an important regulator of keratinocyte and
647 melanocyte differentiation during hair follicle morphogenesis and cycling. Am. J. Pathol. 160,
648 1807-1821.
649 Walzer, C., Schönenberger, N., 1979a. Ultrastructure and cytochemistry study of the yolk syncytial
650 layer in the alevin of trout (*Salmo fario trutta* L.) after hatching. I. The vitellolysis zone. Cell
651 Tissue Res. 196, 59-73.
652 Walzer, C., Schönenberger, N., 1979b. Ultrastructure and cytochemistry of the yolk syncytial layer in
653 the alevin of trout (*Salmo fario trutta* L. and Salmo gairdneri R.) after hatching. II. The
654 cytoplasmic zone. Cell Tissue Res. 196, 75-93.
655 Wallace, R.A., Begovac, P., 1985. Phosvitins in *Fundulus* oocytes and eggs. J. Biol. Chem. 260,
656 11268-11274.
657 Wallace, R.A., Selman, K., 1985. Major proteins changes during vitellogenesis and maturation of
658 *Fundulus* oocytes. Dev. Biol. 110, 492-498.
659 Yajima, Y., Kawashima, S., 2002. Calpain function in the differentiation of mesenchymal stem cells.
660 Biol. Chem. 383, 757-764.
661 Yasothornsrikul, S., Greenbaum, D., Medzihradszky, K.F., Toneff, T., Bundey, R., Miller R.,
662 Schilling, B., Petermann, I., Dehnert, J., Logvinova, A., Goldsmith, P., Neveu, J.M., Lane,
663 W.S., Gibson, B., Reinheckel, T., Peters, C., Bogyo, M., Hook, V., 2003. Cathepsin L in
664 secretory vesicles functions as a prohormone-processing enzyme for production of the
665 enkephalin peptide neurotransmitter. Proc. Natl. Acad. Sci. U.S.A. 100, 9590-9595.
666 Yeh, H.Y., Klesius, P.H., 2008. Molecular cloning, sequencing and characterization of channel catfish
667 (*Ictalurus punctatus*, Rafinesque 1818) cathepsin S gene. Vet. Immunol. Immunopathol. 126,
668 382-387.
669 Yeh, H.Y., Klesius, P.H., 2009. Channel catfish, *Ictalurus punctatus*, cysteine proteinases: cloning,
670 characterisation and expression of cathepsin H and L. Fish Shellfish Immunol. 26, 332-338.
671 Zhang, T., Rawson, D.M., Tosti, L., Carnevali, O. 2008. Cathepsin activities and membrane integrity
672 of zebrafish (*Danio rerio*) oocytes after freezing to -196 degrees C using controlled slow
673 cooling. Cryobiology 56, 138-143.
674

Figure Legends

Fig. 1. Expression of *fhctsb* and *fhctsla* in *F. heteroclitus* embryos at different developmental stages determined by quantitative real-time PCR. Transcript levels of the *F. heteroclitus* ornithine decarboxylase (*odc*) gene were used as reference, and relative transcript levels were calculated as fold change using the $2^{-\Delta\Delta Ct}$ method. Data are presented as means ± SEM ($n = 3$ different batches of embryos). Values with a different superscript are significantly different (Kruskal-Wallis test, $p < 0.05$).

Fig. 2. Expression of *fhctsb* during *F. heteroclitus* early embryogenesis up to the late neurula stage (18-19 somites) at 48 h postfertilization (48 hpf) by whole-mount *in situ* hybridization using antisense DIG-labelled riboprobes (blue color). Lateral views of embryos with rostral to the left (A-C and F-G), and cross-section (D). Transcripts were not detected at morula stage (A) or at 50% epiboly (B). The arrowheads in B indicate the marginal region of the gastrula (Gs). In morula embryos, oil globules (Og) react unspecifically with the alkaline phosphatase substrate precipitating BM purple. At the late neurula stage (C), *fhctsb* expression (arrows) was found in the yolk syncytial layer (YSL) surrounding the yolk sac (Ys). The cross-section (D) and enlarged view of the Ys (E) shows the specific labelling around the nuclei in the yolk syncytium (arrows). The expression in the yolk syncytium is prolonged up to the neurula stage (F). The staining using sense riboprobes was negative in all stages (G shows the negative controls at the neurula stage). Scale bars, 500 μm (A-C, F, G), 100 μm (D, E).

Fig. 3. Immunolocalization of FhCtsb in *F. heteroclitus* embryos at the gastrula stage (50-70% epiboly) by immunofluorescence (A; green color), or at the neurula stage by whole-mount immunocytochemistry (C; brown color). The nuclei of blastomeres (Bl) are stained in blue with DAPI (A and B). Negative controls (B and D) were incubated with the anti-FhCtsb antiserum preadsorbed with the synthetic peptide. At the gastrula and neurula stages a strong immunoreactive signal is noted in the yolk syncytial layer (YSL) nearby the yolk sac (Ys), whereas the enveloping layer (Evl) is negative. Note in A the presence of an oil globule (Og) not stained. Scale bars, 20 μm (A, B), 10 μm (C, D).

Fig. 4. Cathepsin B- (A) and L-like (B) enzyme activity in *F. heteroclitus* embryos at different developmental stage. Data are presented as means ± SEM of 3 separate experiments performed on different batches of embryos. Values with different superscript are significantly different (ANOVA, $p < 0.05$).

Fig. 5. Immunodetection of FhCtsb in *F. heteroclitus* embryos. (A) Representative FhCtsb immunoblot of FhCtsb immunoprecipitated proteins from embryos at different developmental stages as indicated on the top. The same amount of protein (10 μg) was loaded in each lane. The arrowheads point to the position of the preproenzyme (Pre-proFhCtsb), proenzyme (ProFhCtsb), single chain active form (FhCtsbSC), and heavy chain of the double-chain active form (FhCtsbHC). Apparent molecular mass (M_r) values are given in kDa on the left. (B) Ratio of the intensities of the FhCtsbSC/FhProCtsb immunoreactive bands for each embryo stage. Data are mean ± SEM (n = 3 independent immunoblots). Values with different superscript are significantly different (ANOVA, $p < 0.05$).

Fig. 6. Major yolk proteins (YPs) of *F. heteroclitus* embryos at different developmental stages resolved by 15% SDS-PAGE and stained with Coomassie blue R-350. A volume corresponding to 0.025 embryo equivalents was loaded in each lane. The YPs (arrowheads) are named based on their apparent molecular mass after LaFleur et al. (2005). YPs formed during embryo development are in cursive. Apparent molecular mass (M_r) values are given in kDa on the left.

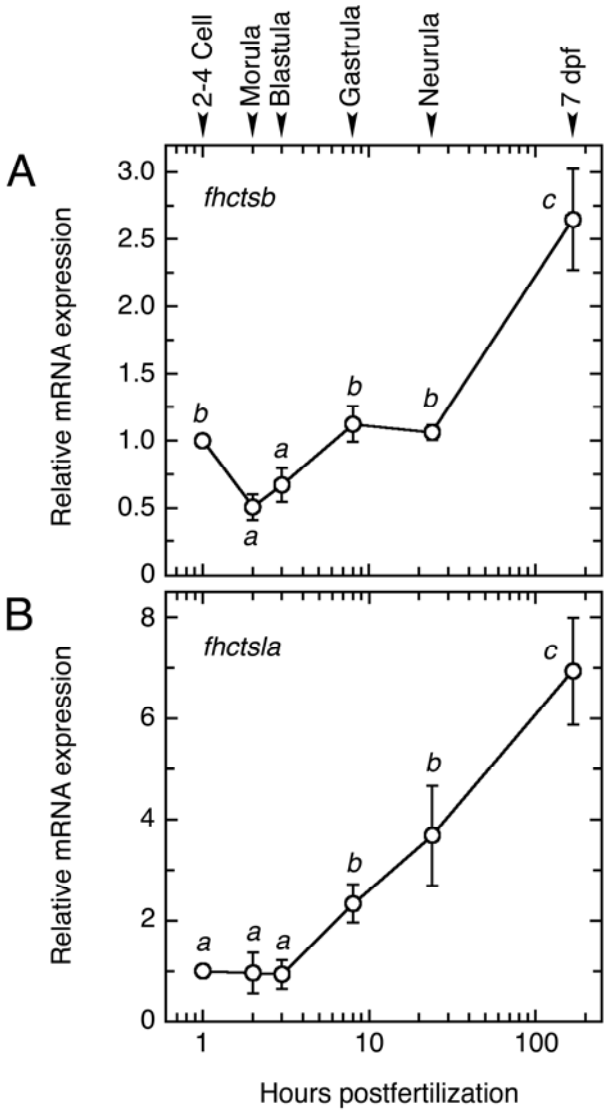
2-4 Cell
Morula
Blastula
Gastrula
Neurula
7 dpf
A
fhctsb
Relative mRNA expression
3.0
2.5
2.0
1.5
1.0
0.5
0
b
a
a
b
b
c
B
fhctsla
Relative mRNA expression
8
6
4
2
0
a
a
a
b
b
c
1
10
100
Hours postfertilization

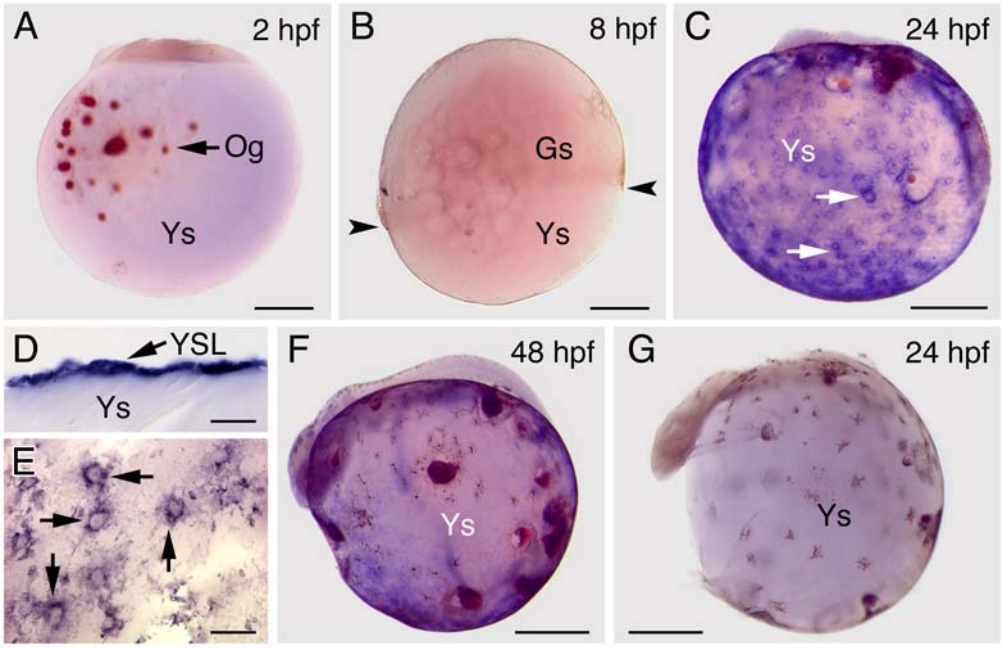
A
2 hpf
Og
Ys
B
8 hpf
Gs
Ys
C
24 hpf
Ys
D
YSL
Ys
E
F
48 hpf
Ys
G
24 hpf
Ys

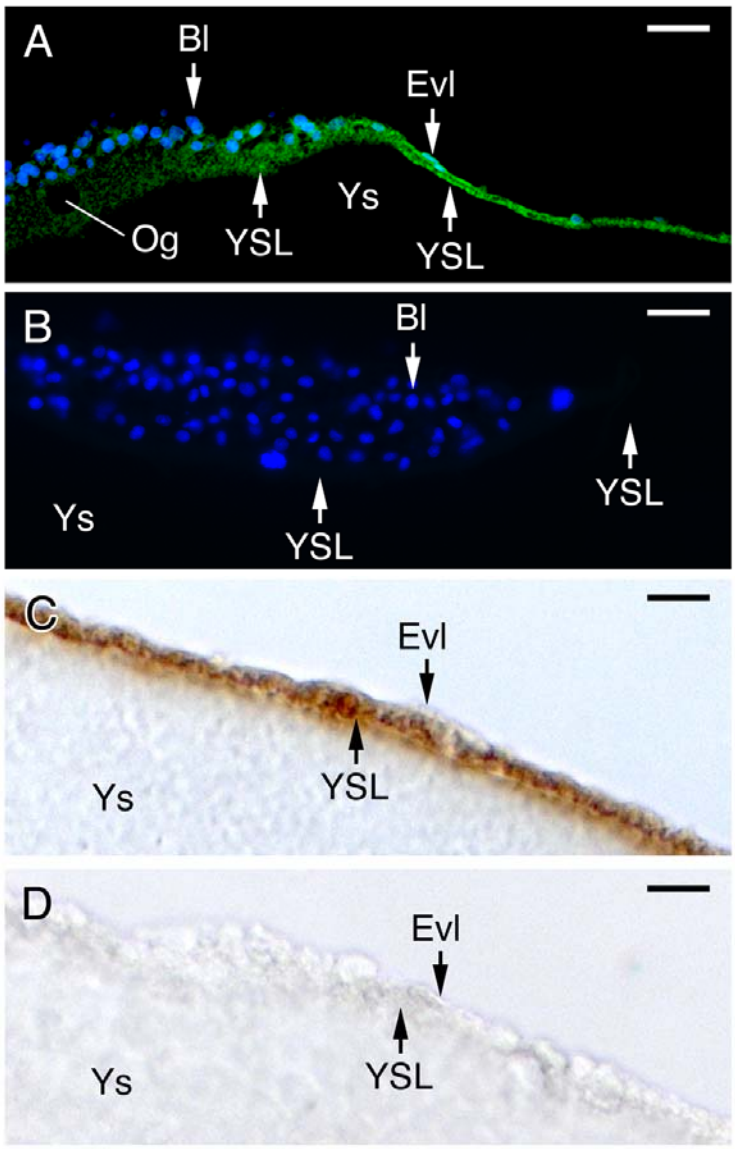
A
Bl
Evl
Ys
Og
YSL
YSL
B
Bl
YSL
Ys
YSL
C
Evl
YSL
Ys
D
Evl
YSL
Ys

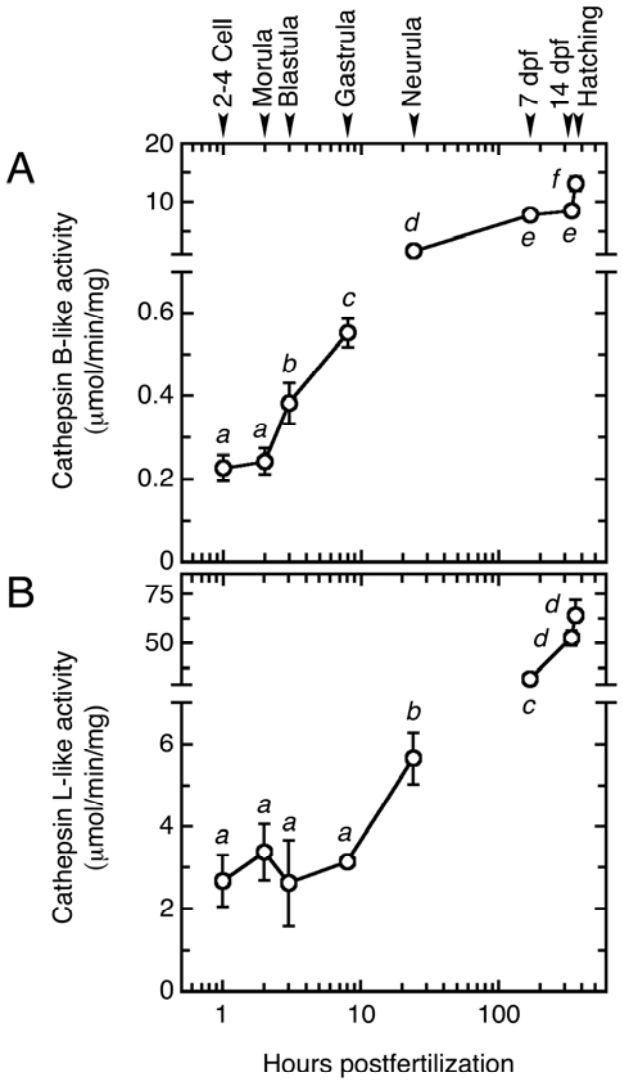
2-4 Cell
Morula
Blastula
Gastrula
Neurula
7 dpf
14 dpf
Hatching
A
Cathepsin B-like activity
(μmol/min/mg)
20
10
0.6
0.4
0.2
0
a
a
b
c
d
e
e
f
B
Cathepsin L-like activity
(μmol/min/mg)
75
50
6
4
2
0
a
a
a
a
b
c
d
d
1
10
100
Hours postfertilization

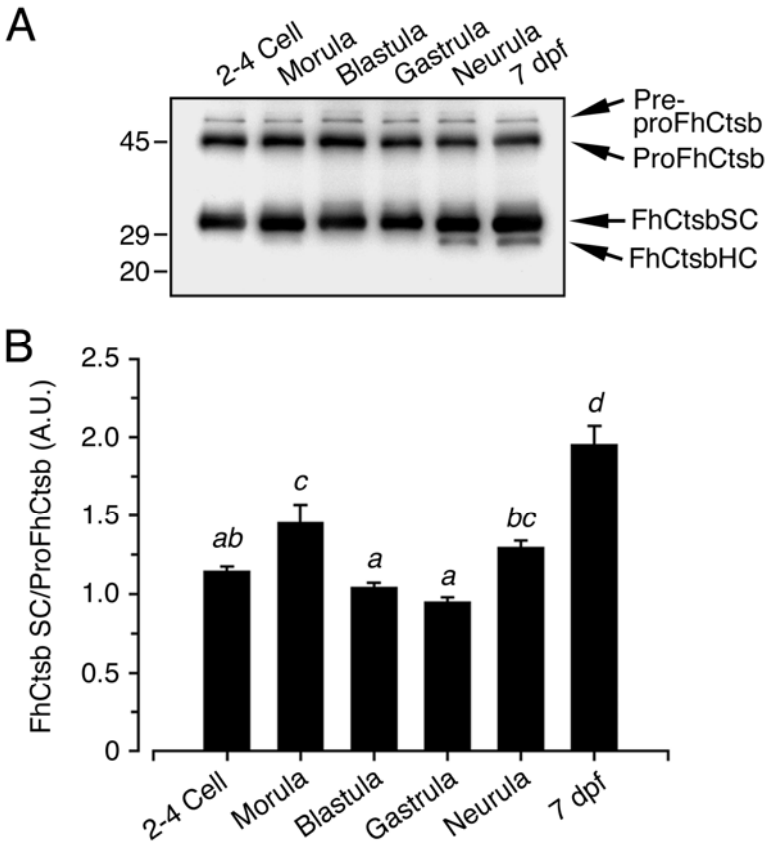
A
2-4 Cell
Morula
Blastula
Gastrula
Neurula
7 dpf
45
29
20
Pre-
proFhCtsb
ProFhCtsb
FhCtsbSC
FhCtsbHC
B
FhCtsb SC/ProFhCtsb (A.U.)
2.5
2.0
1.5
1.0
0.5
0
ab
c
a
a
bc
d
2-4 Cell
Morula
Blastula
Gastrula
Neurula
7 dpf

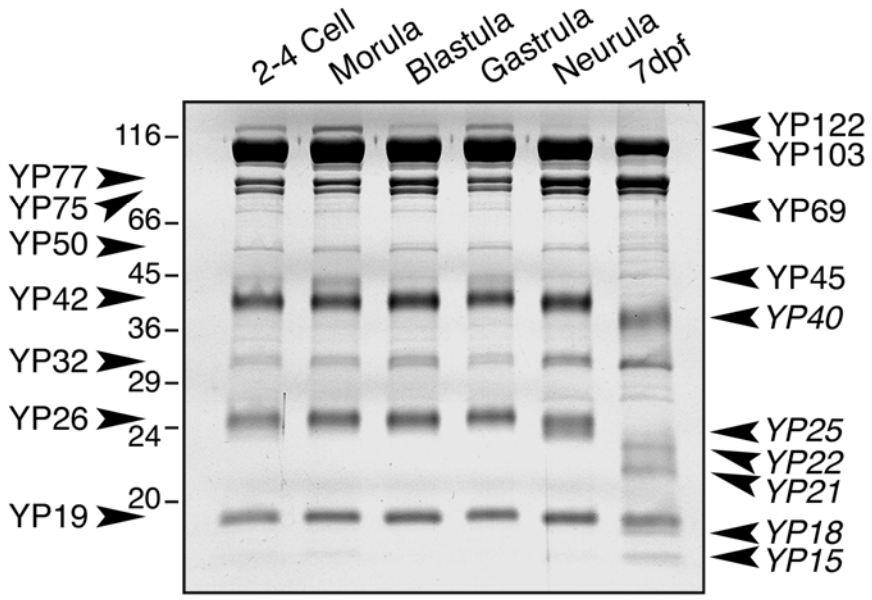
2-4 Cell
Morula
Blastula
Gastrula
Neurula
7dpf
116
66
45
36
29
24
20
YP77
YP75
YP50
YP42
YP32
YP26
YP19
YP122
YP103
YP69
YP45
YP40
YP25
YP22
YP21
YP18
YP15